Microdroplet-Controlled Divergent Reactivity at a Gas-Organic Interface

Boyu Zheng[1†], Linlong Dai[1,2†], Luyun Xue[1], Qing Xu[1], Jiannan Sun[1], Jinhua Liu[1], Xiaofei Zeng[1*], Guofu Zhong[2,3*] and Heyong Cheng[1*]

[1] College of Material, Chemistry and Chemical Engineering, Key Laboratory of Organosilicon Chemistry and Material Technology, Ministry of Education, Hangzhou Normal University, Hangzhou, 311121, Zhejiang, China

[2] Department of Chemistry, Eastern Institute for Advanced Study, Ningbo, 315200, Zhejiang, China

[3] School of Chemistry and Chemical Engineering, Qufu Normal University, Qufu, 273165, Shandong, China

*Corresponding Authors: chemzxf@hznu.edu.cn; guofuzhong@eias.ac.cn; hycheng@hznu.edu.cn; [†]B. Zheng and L. Dai contributed equally to this work.

Abstract

Gas-liquid Interface plays key roles in many fantastic phenomena due to specific properties. Although remarkable reactivities were benefited from gas-water interface of aqueous microdroplets, it remains unknown for gas-organic interface. This work discovers such extraordinary reactivity of gas-organic interface using organic microdroplets (acetonitrile and other organic solvents). This reactivity at the gas-organic interface facilitated a novel microrordroplet-controlled divergence, i.e., double C–N cleavage in high efficiency (yields > 90% in milliseconds) compared to single C–N bond breakdown and intramolecular cycloarrangement in bulk under harsher conditions from the same imidazolines. This study is not only important to wide applicability and inherent mechanisms of the gas-organic interface but also enables good insights into gas-water and other interface-rich studies in atmospheric and photochemistry, on-water chemistry, biological and biomedical, industrial, and energy.

Keywords

Gas-organic interface; interfacial effect; divergent reactivity; chemoselectivity; microdroplets; reaction acceleration; vicinal diamines; *N*-heterocycles

Introduction

The main paragraph text follows directly on here. Interfaces (gas-liquid, gas-solid and liquid-solid) are ubiquitous in nature (aerosol, mist, cell membrane, etc.) and technology (on-water chemistry, electrical double layer, microdroplets, etc.). Among them, gas-liquid interfaces have drawn extensive interests in scientific and engineering community because many fantastic phenomena and processes have been associated with specifically different properties of the interfaces from single phases, i.e., dramatical acceleration of many chemical and photochemical reactions, implying potential applications in atmospheric, biological, biomedical, prebiotic, electrochemical, geochemical, photochemical and synthetic chemistry.[1-7] Despite substantial progress over the past decades, current investigations of gas-liquid interface are limited to aqueous interface, where gas-organic interface remains neglected and our understanding to the fundamental mechanisms and general uses is hence impaired.

Microdroplet chemistry, which takes advantage of the air-liquid interfacial effect of tiny droplets,[8-10] has become a popular tool in various fields such as analysis,[11-14] reaction monitoring,[15-18] organic synthesis,[19-38] and biological[39-43] and environmental[44] studies. While many studies have reported accelerated reactions in microdroplets, the extraordinary reactivities including three-component Mannich-type reactions,[21] hydrolysis of esters,[45] tandem amide formation,[46] the synthesis of gold-histidine complexes,[33] and bromination of 1,2,3-triazoles[34] have realized at the gas-water interface in aqueous microdroplets (pure water or water/organic binary solvents with more than 50% water). However, this extraordinary reactivity remains unexplored at the gas-organic interface, which is highly desirable considering a major use of organic solvents. It is undoubtedly beneficial to uncovering the inherent mechanisms and further broadening the applicability of the unique reactivity of microdroplet chemistry. In addition, the extraordinary reactivity implies a novel possible strategy for divergent reactions[47] other than temperature (Scheme 1A),[48] catalyst type (Scheme 1B)[49-50] and ligand for metal catalysts (Scheme 1C),[51] and solvent strategies (Scheme 1D),[52] which has not been fully understood. In this study, we first discovered the unique reactivity at the gas-organic interface by using organic microdroplets

(in pure organic solvents), and then a novel microdroplet-controlled divergence (vicinal diamine in organic microdroplets and benzofused 7-membered *N*-heterocycle in bulk phase) was developed (Scheme 1E).

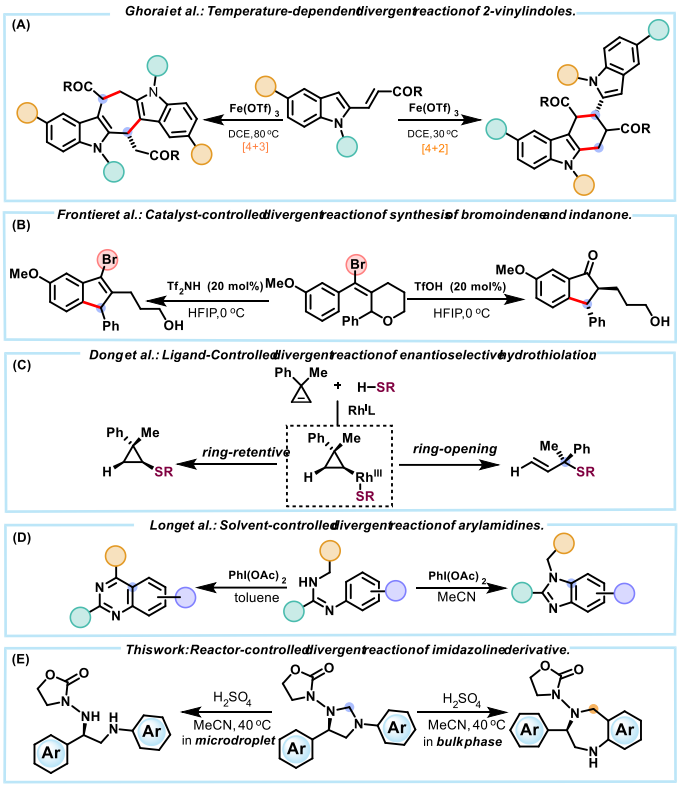

Scheme 1. Divergent reactions depending on the reaction conditions. (A) Temperature-controlled divergent reaction; (B) Catalyst-controlled divergent reaction; (C) Ligand-controlled divergent reaction; (D) Solvent-controlled divergent reaction; (E) Reactor-controlled divergent reaction

1,2-Diamines are important structural motifs in biologically active natural products, pharmaceutical substances, and organic catalysts and ligands.[53-57] Figure 1 illustrates two typical chiral 1,2-diamine-based antibiotics. The construction of 1,2-diamines has attracted much attention in organic community, and considerable methods have been developed for this aim in recent decades.[58-60] Classic methods for synthesizing diamines typically involve i) diamination of olefins,[61-63] ii) reduction of imines,[64-67] iii) nucleophilic addition of imines,[68-69] iv) radical coupling of imines,[70-71] and v)

Mannich-type reactions.[72-74] 1,4-Benzodiazepines with a main skeleton of benzofused *N*-heterocycles are important drugs to relieve insomnia and anxiety, and also to treat muscle spasm and prevent seizures.[75] Benzofused *N*-heterocycles can be constructed from i) ring expansion of 1,3-diaza-heterocycles via aryne insertion into a C(sp^3)–N σ-bond,[76] ii) cyclization reaction of *N*-(chloroacetyl)-2-aminobenzophenone derivatives with hexamethylenetetramine in the presence of NH_4OAc,[77] iii) deprotection and cyclization after Ugi-4CR route,[75, 78] and iv) one-pot reaction of *N*-carboxyanhydrides and *o*-ketoanilines promoting benzodiazepine formation with a two-stage process.[79] In this work, we presented a simple, green and high-efficient strategy to construct vicinal diamines and benzofused *N*-heterocycle from the same imidazoline precursor using two different reactors (vicinal diamines by microdroplets and benzofused *N*-heterocycle by bulk counterpart) (Scheme 1E).

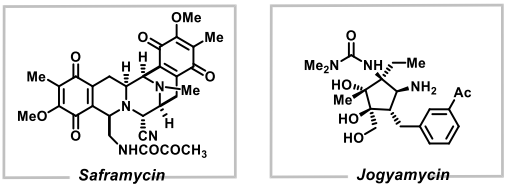

Figure 1. Selected examples of chiral 1,2-diamine-based biologically active molecules of antibiotics.

C–N bond is a key and universal structural skeleton in thousands of natural products, which has a decisive impact on the biological properties of drug molecules.[80] The "inside-outside" C–N bond could be broken selectively under different catalytic conditions, and new multi-purpose and high-performance arylation/acylation/transamination reagents were developed (Scheme 2A).[81] In 2020, the imidazolidinone ring of 1,3-dihydro-1*H*-benzimidazol-2-one was opened by Ph_3P-I_2, and the C–N bond in the five membered ring was broken to form aryliminophosphoranes (Scheme 2B).[82] However, the C elements of these broken C–N bonds were all connected with carbonyl functional groups, while the relevant research on N–C–N bond cleavage is rare. Imidazolines, basically a partially saturated

analog of imidazole, are high-value in medical, pharmaceutical, laundry and other uses. Ring opening of imidazoline has been used to study the ring-chain tautomerism of 1,3-disubstituted diazolidines under acidic conditions (Scheme 2C).[83-84] However, double cleavage of carbon-nitrogen bonds of imidazoline compounds has never been reported.

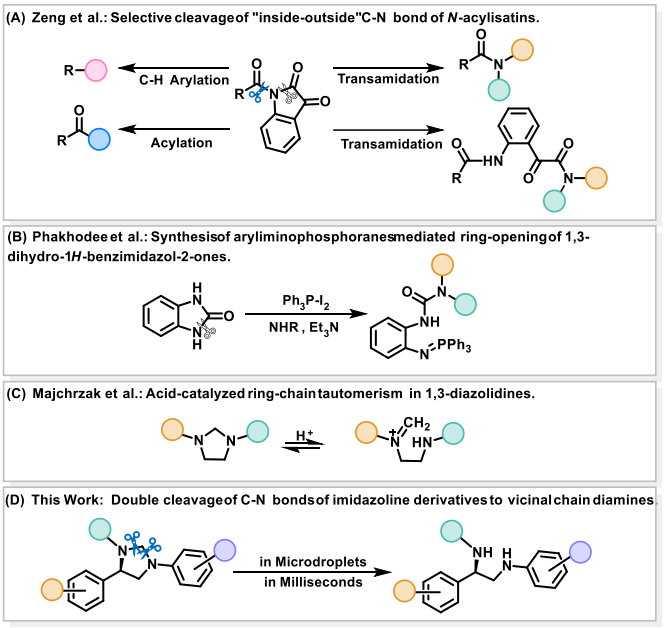

Scheme 2. Different strategies for the cleavage of C–N bond. (A) Selective cleavage of "inside-outside" C–N bond; (B) Selective cleavage of inside C–N bond; (C) Ring-chain tautomerism; (D) Double cleavage of C–N bonds

Herein we reported a novel pathway to form 1,2-diamines by the on-pot double cleavage of two C–N bonds in imidazoline derivatives (Scheme 2D). In comparison with previous method for constructing diamines, the proposed pathway in this work is simple, high-efficient, and mild. Moreover, the double C–N bond breakdown for the construction of vicinal diamines was the first example of extraordinary reactivities of organic microdroplet chemistry (Scheme 3). Five membered ring of an imidazoline derivative 1a was opened chemoselectively only in organic microdroplets, in which two C–N bonds

were broken in one pot to form vicinal diamines in milliseconds. Instead, two different products, majorly benzofused 7-membered N-heterocycle 3a from rearrangement of a ring-open intermediate and minorly imine 4a were offered in bulk phase under harsh conditions after overnight reaction.

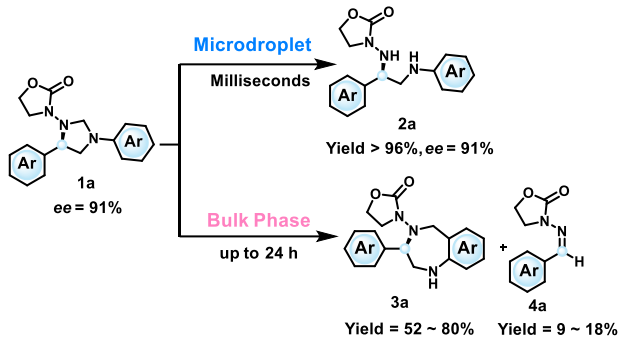

Scheme 3. Ring opening of imidazoline derivative 1a to generate vicinal diamine in microdroplet and benzofused 7-membered *N*-heterocycle and imine in bulk phase.

Experimental Methods

Full experimental details, including general information, experimental methods for ring opening reactions and rearrangement reactions, reaction optimization, mechanistic studies, Chiral studies, ^{1}H NMR spectra, ^{13}C NMR spectra, high-resolution mass spectrometry (HRMS) and High-performance liquid chromatography (HPLC) data are available in the supplemental information for all compounds. Crystallographic data are available free of charge from the Cambridge Crystallographic Data Centre (CCDC): 2235405. Raw data are available from the corresponding author upon reasonable request.

Double C–N cleavage in organic microdroplets: Imidazoline derivative 1 (1.5 mg, 5.0 mmol L^{-1}, 1.0 equiv) and 0.05–5 µL (0.18–18.4 equiv) of sulfuric acid (98%) were dissolved in 2 mL acetonitrile. The mixed solution was fed (15-300 µL min^{-1}) into a concentric capillary (150 µm ID × 365 µm OD) of a nebulizer with dry nitrogen gas

at 101.5 psi. Microdroplets were sprayed into an electrically heated glass chamber with temperature monitored by a thermocouple thermometer, and collected in a 25 mL glass beaker for 10 min (Figure S1). The collected crude product was washed with saturated aqueous $NaHCO_3$ and extracted with dichloromethane (1 mL). The organic layer was collected and filtered by a 0.22 μm filter, and appropriately diluted for yield measurements by high performance liquid chromatography (HPLC) using external standard method. The crude product from scaled reaction was purified by preparative thin-layer chromatography (PTLC) (petroleum ether / ethyl acetate = 3 : 1 ~ 1 : 1) for characterization.

Rearrangement reactions in bulk phase: Imidazoline derivative 1 in acetonitrile (1.5 – 15 mg, 5 – 50 mmol L^{-1}, 1.0 equiv) and sulfuric acid (98%, 2.3 – 18.4 equiv) were mixed in glass bottles and stirred vigorously in a water bath for 10 min to 24 h. The reaction solution was concentrated to dryness, washed with saturated aqueous $NaHCO_3$ and extracted with dichloromethane. Rearranged product benzofused 7-Membered *N*-Heterocycles 3 in the organic phase was purified by PTLC (petroleum ether / ethyl acetate = 3 : 1 ~ 1 : 1) for HPLC analysis and structural characterization.

Results and Discussion

Organic Microdroplet Chemistry Driving Different Reaction Pathways from Bulk Phase

(*R*)-3-(3,5-Diphenylimidazolidin-1-yl)oxazolidin-2-one 1a was utilized as the model substance for investigating different reactivities in organic microdroplets and bulk phase. The reactant 1a (5 mmol L^{-1}) and sulfuric acid (11 mmol L^{-1}) was prepared in acetonitrile. The prepared reaction solution was then introduced into a sonic sprayer to generate organic microdroplets at a flow rate of 15 μL min^{-1}, and the resulted product from the sprayed microdroplets was collected for 10 min (see the setup in Figure S1). After exaction with dichloromethane and washing with aqueous sodium bicarbonate, the organic phase was analyzed by HPLC for estimating reaction yields. As shown in Figure 2A, a vicinal diamine product 2a was generated in the microdroplet reactor due to double C–N bond cleavage of 1a, where formaldehyde was formed from the

eliminated methylene group (see a plausible reaction mechanism in Scheme 5). We further carried out this conversion under various reaction conditions 1a concentration (5-100 mmol L^{-1}), sulfuric acid equivalent (0.18-36.8 equiv.), spray flow rate (5-300 μL min^{-1}), reaction temperature (25-60 °C) and organic solvents, see the details in the following optimization section), and all these microdroplet reactions offered the same product 2a with only difference in reaction yields. In addition, the product 2a formed by organic microdroplet chemistry was in high stereoselectivity (91% *ee*) (see the chirality estimation in supporting information S9), which is attractive to the discovery of chiral drugs.

We followingly performed this conversion in bulk phase for comparison purpose. The reactant 1a stirred in a bulk solution was unreacted within 10 min. After one hour reaction in bulk, a different product, benzofused 7-membered *N*-heterocycle 3a from rearrangement of a ring-open intermediate was surprisingly formed in addition to a trace amount of 2a (Figure 2B). When the bulk reaction was continued overnight, the benzofused *N*-heterocycle 3a was dominant as well as a minor imine 4a (Figure 2C). Moreover, the benzofused *N*-heterocycle 3a was in high stereoselectivity (Figure S2). Chemical structures of the benzofused *N*-heterocycle 3a and imine 4a were characterized by proton and carbon nuclear magnetic resonance spectroscopy (Figure S38-S40), high-resolution mass spectrometry (Figure S43-S44) and X-radiation diffractometer (Figure 2C & Figure S2). The monitoring of the bulk reaction demonstrated that the yields of the benzofused *N*-heterocycle product 3a and imine 4a were gradually improved (Figure S3). We further investigated this conversion in bulk phase under different conditions. The results (Figure S3 d&f) demonstrated high reaction temperature and large sulfuric acid equivalent were favorable to the rearrangement pathway, and best conversions near to 80% was obtained within 4 hours when the bulk reaction was assisted by 18.4 equiv. sulfuric acid at 60 °C.

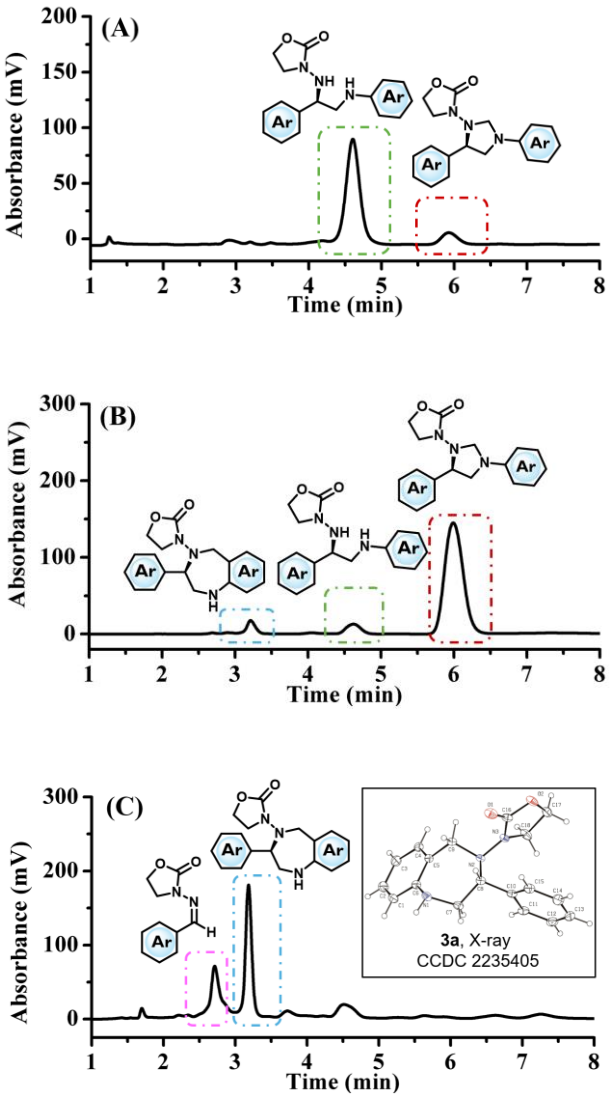

Figure 2. High performance liquid chromatograms of the crude products collected from different reactors using 1a as reactant under the same conditions. (A) Reacting in microdroplet reactor for ten minutes. (B) Reacting in bulk reactor for one hours. (C) Reacting overnight in bulk reactor.

The above results demonstrated different reaction pathways of the imidazoline derivative 1a in Scheme 3. Considering the extraordinary performance of water microdroplets in driving different reaction pathways from its bulk counterpart in the previous works,[21, 33-34, 45-46] we performed several control experiments to elucidate whether aqueous or organic microdroplets drives the chemoselective double C–N cleavage. We first

compared the microdroplet reaction of the imidazoline derivative 1a in chromatographic and anhydrous acetonitrile with trifluoromethanesulfonic acid (with the similar catalytic performance to sulfuric acid, see Entry 2 in Table 1) as the acidic catalyst to avoid trace water from concentrated sulfuric acid and acetonitrile, and the result demonstrated no observable yield variations. we next monitored the double C–N breakdown of the imidazoline derivative 1a in aqueous microdroplets upon the introduction of water into acetonitrile. The result (Table 1, Entries 13-14) demonstrated that the double C–N cleavage was moderately retarded when more water was introduced. Similarly, the introduction of water into the reaction solution did not switch the reaction pathways in bulk although the conversion of 1a to 3a and 4a was prolonged as well as low conversion ratios (Figure S4). A further screening of organic solvents demonstrated that the chemoselective double C–N cleavage of 1a can be realized by organic microdroplets by using all tested organic solvents (see the solvent optimization in Table S5, Entries 1-6). It confirmed that the chemoselective double C–N bond decomposition to form the vicinal diamine product 2a was driven by organic microdroplets rather than aqueous microdroplets. In other words, our study proved the strong power of organic microdroplet chemistry in driving extraordinary reactions as similar as aqueous microdroplet chemistry for the first time.

Optimization of Reaction Conditions

Although the reaction pathway in organic microdroplets has been proved different from the bulk phase, the conversion ratios for the two main products 2a and 3a was far away from quantitative synthesis, leading to a necessity to careful optimization of reaction conditions.

Six acid catalysts (sulfuric acid, trifluoromethanesulfonic acid, phosphoric acid, hydrochloric acid, acetic acid and trifluoroacetic acid) were first screened for the acid-catalyzed ring opening in organic microdroplets. As demonstrated in Table 1 (Entries 1-4) and Table S2, sulfuric acid and CF_3SO_3H were the two suitable acid catalysts for this conversion, and sulfuric acid was selected considering its slight better performance than the latter. An optimization of catalyst loading amount was carried out in the following. As the loading amount of

sulfuric acid was increased from 18 mol% to 184 mol%, the yield of 2a by organic microdroplets was significantly improved up to 90% (Table 1, Entries 7-9, and Table S3). The microdroplet reaction was hardly affected on further increasing sulfuric acid to 36.8 equivalents (Table S3). For comparison, no vicinal diamine 2a can be synthesized without the catalysis of sulfuric acid (Table S3, Entry 1). The optimization of catalyst loading amount indicated that sulfuric acid equivalent was very important for the ring opening reaction of imidazoline derivative 1a. A moderate loading amount of 2.3 equiv. sulfuric acid was selected considering both good yield and low catalyst consumption.

Effect of reaction solvent on the synthesis of vicinal diamine 2a in microdroplets was thereafter explored following the optimization of the acid catalyst. The results (Table 1, Entries 10-12, and Table S4) demonstrated that the ring opening of 1a by microdroplet chemistry can be realized in all of the tested organic solvents except that 1a was insoluble in methanol. Among the six tested organic solvents, acetonitrile (MeCN), dichloromethane (DCM) and acetone were three of the best solvents for the conversion by organic microdroplets (Table S4, Entries 1-3) whereas tetrahydrofuran (THF) and ethyl acetate (EtOAc) offered comparable yields of vicinal diamine 2a (Table S4, Entries 4-5). In addition, the introduction of a moderate amount of water into acetonitrile as a reaction solvent led to a gradually decreased yield of 2a (Table 1, Entries 13-14) and 3a for both microdroplet and bulk reactor. However, the addition of water did not alter the reaction pathways of the microdroplet and the bulk reactor. Acetonitrile was selected as the reaction solvent considering good yield and low cost.

After the solvents screening, we explored the effect of temperature on the microdroplet reaction in the range of 25-50 °C (Table 1, Entries 15-16, and Table S5). The experimental results demonstrated the synthesis of vicinal diamine 2a was slightly improved on enhancing the temperature for the microdroplet ring opening reaction. A moderate temperature of 40 °C was considered considering high yield and low energy consumption.

Table 1. Screen of reaction parameters for ring opening of imidazoline derivative (1a) in microdroplets.

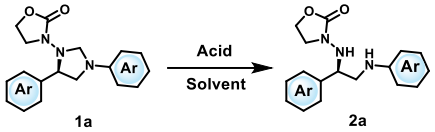

Entry	Acid (equiv.)	Solvent	Temperature (°C)	Yield (%)
1	H_2SO_4 (18.4)	MeCN	40	96
2	CF_3SO_3H (18.4)	MeCN	40	89
3	H_3PO_4 (18.4)	MeCN	40	25
4	CF_3COOH (18.4)	MeCN	40	7
5	H_2SO_4 (4.6)	MeCN	40	94
6	H_2SO_4 (2.3)	MeCN	40	93
7	H_2SO_4 (1.8)	MeCN	40	90
8	H_2SO_4 (0.92)	MeCN	40	75
9	H_2SO_4 (0.18)	MeCN	40	38
10	H_2SO_4 (2.3)	EtOAc	40	76
11	H_2SO_4 (2.3)	DCM[a]	40	93
12	H_2SO_4 (2.3)	DMSO	40	24
13	H_2SO_4 (2.3)	10% H_2O-MeCN	40	86
14	H_2SO_4 (2.3)	50% H_2O-MeCN	40	60
15	H_2SO_4 (2.3)	MeCN	25	81
16	H_2SO_4 (2.3)	MeCN	50	95

Standard reaction conditions: 0.005 mol L^{-1} imidazoline derivative 1a and 2.3 equiv. H_2SO_4 were added in 1 mL different solvents; microdroplets were sprayed at 15 µL min^{-1} by N_2 under 101.5 psi at different temperature and were collected in a 25 mL glass beaker for 10 min. [a]10% MeCN-DCM was used as the solvent for good dissolvement.

Scope of Imidazoline Derivatives

The success of chemoselective synthesis of vicinal diamine 2a by the accelerated microdroplet ring opening reaction prompted us to explore the scope of imidazoline derivatives including six imidazoline reactants 1b-1g bearing electron-attracting and donating groups (methyl, trifluoromethyl, fluoro, and phenyl) on the meta-/para positions of the two phenyl cycles with similar motifs to the model reactant 1a (see the synthesis of these starting materials in S2). The ring opening reactions of these imidazoline derivatives were carried out under the above optimized conditions unless stated else, and the yields measured by HPLC are listed in Scheme 4. Three conclusions can be drawn from the result in Scheme 4. First, all of the imidazoline derivatives can be chemoselectively converted into their corresponding vicinal diamines 2 with satisfactory yields (> 90%) by organic microdroplet chemistry. In contrast, the rearrangement benzofused *N*-heterocycle products 3b-3d and 3f-3h can be chemoselectively produced with moderate yields (31%~69%) in the bulk reactions (proton and carbon nuclear magnetic resonance spectra in Figure S41-S52, and high-resolution mass spectra in Figure S57-S62). It further confirmed the specific role of organic microdroplet chemistry in driving different reactivity from its bulk counterpart. Second, the reaction efficiency by organic microdroplet chemistry was improved by at least four orders of magnitude relative to the bulk as evidenced from a rough comparison between reaction times (less than 1 ms in microdroplets versus > 12 hours in bulk). Considering the yield superiority of organic microdroplet chemistry (> 90%) over the bulk (< 60%), the reaction efficiency may be further enhanced by organic microdroplet chemistry. Last, neither electron-donating nor electron-attracting substituted groups born by the imidazoline derivatives 1 had observable interfering effect on the ring opening reaction by the microdroplet method. However, the rearrangement reaction in bulk was moderately affected when the *N*-phenyl of imidazoline derivatives were para-substituted. To further demonstrate the feasibility of the chemoselective synthesis by organic microdroplet chemistry and the bulk, a general imidazoline derivative reactant 1h was also tested. The microdroplet reaction can still proceed smoothly to quantitatively yielding the vicinal diamine product 2h by using the reactant 1h (Scheme 4, Entry

8), and the bulk reaction also chemoselectively generated the rearrangement product 3h with a moderate yield (47%). These results proved the advantages of organic microdroplet chemistry including high reaction selectivity, high reaction efficiency and wide substrate scope, showing considerable application potential in organic synthesis.

Scaled-up for Synthesis of Vicinal Diamine in Microdroplets

In spite of reaction acceleration driven by microdroplet chemistry, low product amount in microdroplets limits its application in organic and industrial synthesis. At present, three strategies have been adopted to scale up microdroplet reaction, namely, array sprayers,[23, 85-86] high flux[24-25, 33, 87] and solvent recycling.[26] In this experiment, high flux strategy was used to scale up the synthesis of vicinal diamine 1a in microdroplets due to its simplicity. The amount of vicinal diamine 2a was amplified by increasing the concentration of substrate 1a and the flow rate of the reaction solution. As the reaction yield by organic microdroplet chemistry may be reduced under the standard reaction conditions by using the high flux strategy, the temperature and the sulfuric acid equivalent may be enhanced to improve the yield of vicinal diamine 2a in the scaled-up. As shown in Table S6, when the substrate 1a was ten-fold concentrated (0.05 mol L^{-1}), the amount of the vicinal diamine 2a was enhanced by nearly ten times although the yield of this reaction was not good as the microdroplet reaction under the standard conditions (0.005 mol L^{-1} 1a). When the microdroplet reaction was carried out at a raised temperature (50 °C), the amount of the vicinal diamine 2a was further enhanced by upscaling the flow rate of reaction solution to 300 μL·min^{-1} (Table S6, Entries 2-6). For example, a product 2a amount of approximately 3.0 mg min^{-1} (177 milligrams per hour) can be obtained by using 0.05 mol L^{-1} imidazoline derivative 1a at 300 μL min^{-1} (Table S6, Entry 6). When the concentration was continued to increase to 0.1 mol L^{-1}, the yield was good at low flow rates (15 μL·min^{-1}) but was sharply decreased at high flow rates (Table S6, Entries 7-9). It indicated that the high flux strategy was incapable to further scale up the microdroplet reaction (at most 177 mg h^{-1}). By utilizing the array sprayers[23, 85-86] and solvent recycling strategies,[26] it is anticipated to readily enlarge the product amount to several grams per hour.

Scheme 4. Ring opening reaction yields of different imidazoline derivatives in microdroplets and bulk phase.

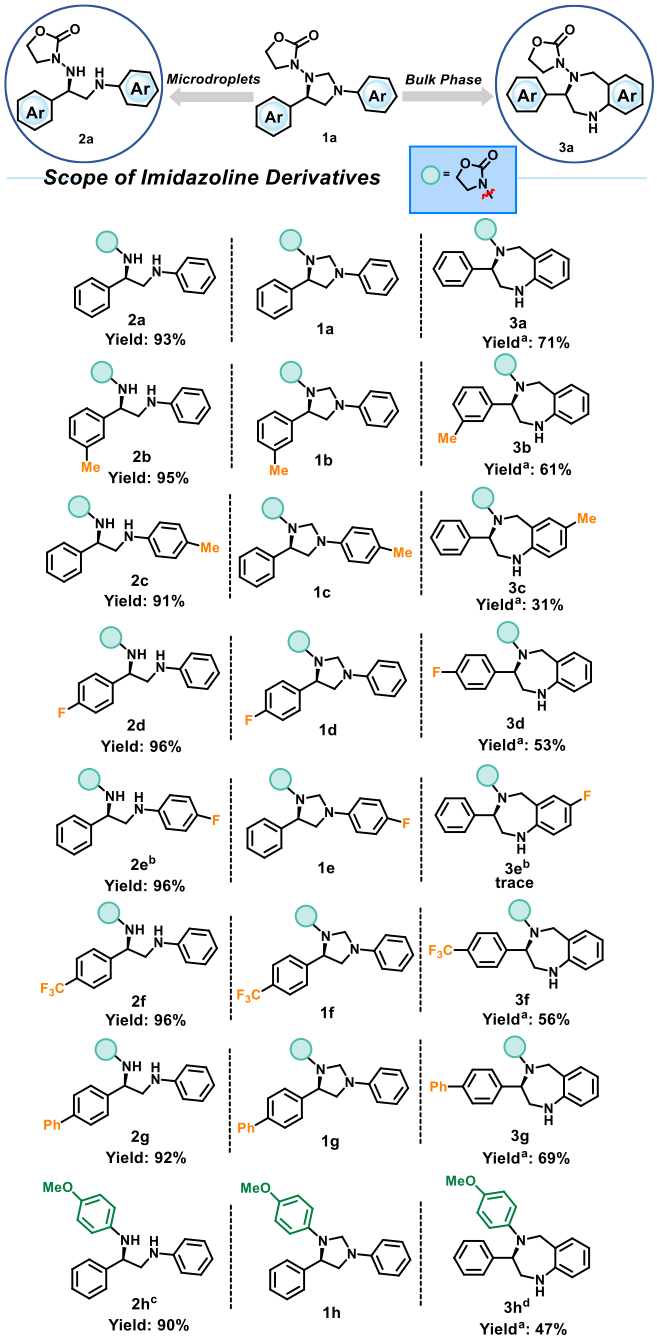

Microdroplet reaction conditions: 0.005 mol L^{-1} imidazoline derivatives 1 and 2.3 equiv. H_2SO_4 were added in 1 mL MeCN or THF; microdroplets were sprayed at 15 μL min^{-1} by N_2 under 101.5 eq at 40 °C and were collected in a 25 mL glass beaker for 10 min. [b]THF was used as the solvent. [c]THF was used as the solvent and only 1.8 equiv. H_2SO_4 was used as catalyst.

Bulk Reaction conditions: 0.025 mol L^{-1} imidazoline derivatives 1 and 18.4 equiv. H_2SO_4 were added in 2 mL MeCN or THF and the solution was stirred vigorously at 60 °C for 12 h. [a]Yield of isolated 3. [b]THF was used as the solvent. [d]THF was used as the solvent and only 3.68 equiv. H_2SO_4 was used as catalyst. The reaction time was increased to 24 h.

Reaction Mechanism for Ring Opening in Organic Microdroplets and Rearrangement in Bulk

Ring-chain tautomerism in 1,3-disubstituted diazolidines has been proved an acidic catalyzed ring opening process.[83] Chain form of 2-aryl-substituted 1,3-diazolidines can be stabilized by the resonance of positive charge on the aryl ring, leading to the removal of benzaldehyde due to the nucleophilic attack of water on the double bond of chain imines under the flux of trifluoroacetic acid.[84] These previous studies shed light on possible reaction mechanisms of different reaction pathways in microdroplets and bulk phase in this work.

We first tried to figure out if methylene was eliminated as formaldehyde in the microdroplet-driven double C–N breakdown by using high-resolution mass spectrometry (HR-MS). Due to low ionization efficiency of formaldehyde in electrospray ionization, dansyl hydrazine was utilized as a high-efficiency derivatization agent.[88-89] A formaldehyde standard and two crude collected solutions from the microdroplet and bulk reactions were offline reacted with dansyl hydrazine in 1% acetic acid acidic methanol prior to HR-MS detection. As shown in Figure S7 a&b, the hydrazone product of formaldehyde with dansyl hydrazine was clearly detected as its protonated form at *m/z* 278.0953 (mass error 1.80 ppm), and the abundance ratio of hydrazone to dansyl hydrazine (*m/z* 266.1) from the collection solution by the microdroplet reaction was apparently higher than the formaldehyde standard. As a comparison, the hydrazone peak detected from the reaction mixture of bulk phase after 8 hours reaction was much lower than its microdroplet counterpart. In addition, two additional peaks at m/z 298.1 (corresponding to the protonated vicinal diamine product 2a) and 310.1 (corresponding to protonated imidazoline derivative 1a and rearranged benzofused *N*-heterocycle 3a) were detected from the collection solutions of both microdroplet and bulk reactions, and the abundance ratio of the two peaks by the microdroplet reaction was significantly higher than the bulk reaction. These MS results not only confirmed the elimination of methylene in the form of formaldehyde but indicated different reaction pathways driven by organic microdroplet chemistry in higher efficiency than its bulk counterpart. We also performed a control experiment to check how the imine product 4a was formed. Purified vicinal diamine 2a and rearrangement benzofused *N*-heterocycle 3a were individually stirred in acidic acetonitrile (18.4 equiv.

sulfuric acid) at 60 °C for 12 hours. The two stirred solutions were extracted with dichloromethane and washed with aqueous sodium bicarbonate, and then analyzed by HPLC. As shown in Figure S6, the vicinal diamine 2a was almost completely converted into the imine 4a whereas the rearrangement benzofused *N*-heterocycle 3a was intact. In addition, we also detected aniline by using HR-MS (Figure S8) when vicinal diamine 2a was transformed into the imine 4a. This control result indicated that the imine 4a was produced from the small amount of vicinal diamine 2a in the presence of sulfuric acid under thermal irradiation in the bulk phase.

Scheme 5. Possible mechanism of ring opening reactions in microdroplets and bulk phase

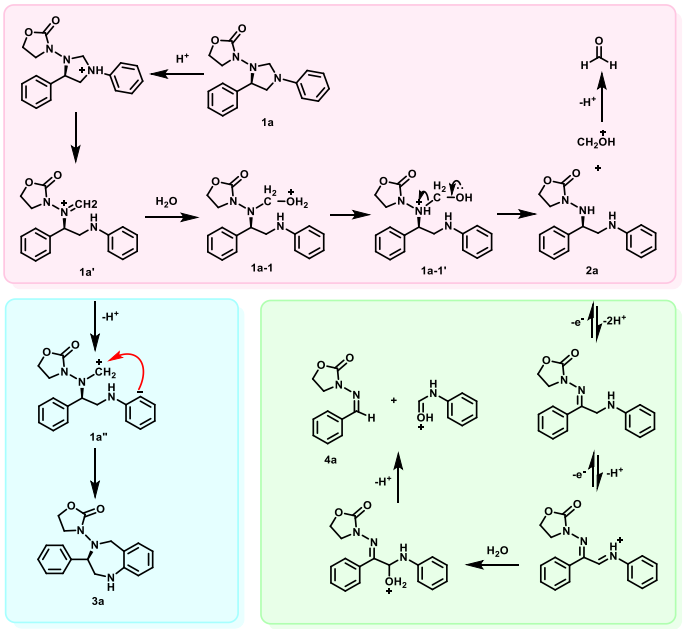

A plausible reaction mechanism (Scheme 5) may be drawn based on the above experimental results. Briefly, a chain iminium cation 1a' was formed by ring opening of the ring imidazoline derivative 1a under sulfuric acidic catalysis. In microdroplets, the chain iminium 1a' was nucleophilically attacked by water on the iminium double bond to form a water coalescent intermediate 1a", and the latter may undergo proton transfer from oxygen to nitrogen and C–N bond cleavage to generate the final

product 2a with elimination of protonated formaldehyde (finally deprotonated to formaldehyde). In bulk phase, the chain iminium 1a' may undergo resonance of the iminium double bond to form a carbocationium intermediate 1a", which may further electrophilically be attack by the adjacent arene carbon and form a benzofused 7-membered *N*-heterocycle product 3a after dehydrogenation. In addition, vicinal diamine 2a may undergo a series of oxidation and nucleophilic attack of the iminium double bond by water in bulk phase, and finally form the imine product 4a by the elimination of the substituted (phenylamino)hydroxymethyl. It should be noted that more studies should be undertaken to uncover the inherent mechanism on how organic microdroplets drive the different reaction pathways.

Gas-liquid interface of microdroplets leads to huge differences from the bulky reactor to drive reaction acceleration and even novel reaction pathways including enthalpy effects of partial solvation, entropy effects, fast solvent evaporation, fast diffusion, ultrahigh electric field, extreme pH, etc.[8-10] We speculated that extremely low pH of microdroplets in this study facilitated the protonation of the imidazoline 1a. Protonated 1a and cationic intermediates (1a’ and 1a-1) may be ordered oriented at the interface to decrease the entropy due to electrostatic repulsion,[39-40] facilitating the thermodynamically unfavorable C–N cleavage of 1,3-diazolidine (a barrier of 16.9 kcal mol^{-1}[83]). It needs to be investigated more in the future to exactly uncover the mechanisms inherent from the gas-liquid interface leading to this extraordinary reactivity in both organic and aqueous microdroplets from more emerging examples. Notably, these remarkable reactivities may also be helpful to other interface-rich studies such as aerosol chemistry,[2] on-water chemistry,[1] biomedical,[4] industrial,[5] and energy.[7]

Conclusion

In conclusion, this study demonstrates that the remarkable reactivity at the gas-liquid interface extends beyond aqueous systems and is applicable to organic systems. Utilizing chemoselective double C–N cleavage, eight imidazoline derivatives were efficiently converted into vicinal diamines in microdroplets, while benzofused 7-membered *N*-heterocycles and minor imines were synthesized in bulk phase. A high flux approach enabled scaling up of the production of vicinal diamines to 177 mg per hour. By employing different synthetic methodologies for the same precursor, this study highlights the versatility of microdroplet chemistry for the discovery of novel molecules with high reaction selectivity, efficiency, substrate scope, and scalability in different reactors. The remarkable reactivity at the gas-organic interface enables good insights into gas-water and other interface-rich studies in atmospheric and photochemistry, on-water chemistry, biological and biomedical, industrial, and energy.

Supporting Information

Supporting Information is available and includes ^{1}H NMR spectra, ^{13}C NMR spectra, high-resolution mass spectrometry (HRMS), High-performance liquid chromatography (HPLC) and Crystallographic data.

Conflict of Interest

There is no conflict of interest to report.

Funding Information

This research was made possible as a result of a generous grant from the financial support from the National Natural Science Foundation of China under project Nos. 22074027, 21976048 and 22171064.

Preprint Statement (required, if applicable)

Research presented in this article was posted on a preprint server prior to publication in CCS Chemistry. The corresponding preprint article can be found here: (DOI; Direct Link)

Acknowledgments

The authors acknowledge the financial support from the National Natural Science Foundation of China under project Nos. 22074027, 21976048 and 22171064.

References

1. Ruiz-Lopez, M. F.; Francisco, J. S.; Martins-Costa, M. T. C.; Anglada, J. M., Molecular reactions at aqueous interfaces. *Nat. Rev. Chem.* **2020,** *4*, 459-475.

2. Zhong, J.; Kumar, M.; Francisco, J. S.; Zeng, X. C., Insight into chemistry on cloud/aerosol water surfaces. *Acc. Chem. Res.* **2018,** *51*, 1229-1237.

3. Björneholm, O.; Hansen, M. H.; Hodgson, A.; Liu, L.-M.; Limmer, D. T.; Michaelides, A.; Pedevilla, P.; Rossmeisl, J.; Shen, H.; Tocci, G.; Tyrode, E.; Walz, M.-M.; Werner, J.; Bluhm, H., Water at Interfaces. *Chem. Rev.* **2016,** *116*, 7698-7726.

4. Chao, Y.; Shum, H. C., Emerging aqueous two-phase systems: from fundamentals of interfaces to biomedical applications. *Chem. Soc. Rev.* **2020,** *49*, 114-142.

5. Davidovits, P.; Kolb, C. E.; Williams, L. R.; Jayne, J. T.; Worsnop, D. R., Update 1 of: mass accommodation and chemical reactions at gas−liquid interfaces. *Chem. Rev.* **2011,** *111*, PR76-PR109.

6. George, C.; Ammann, M.; D'Anna, B.; Donaldson, D. J.; Nizkorodov, S. A., Heterogeneous photochemistry in the atmosphere. *Chem. Rev.* **2015,** *115*, 4218-4258.

7. Ji, Y.; Yin, Z.-W.; Yang, Z.; Deng, Y.-P.; Chen, H.; Lin, C.; Yang, L.; Yang, K.; Zhang, M.; Xiao, Q.; Li, J.-T.; Chen, Z.; Sun, S.-G.; Pan, F., From bulk to interface: electrochemical phenomena and mechanism studies in batteries via electrochemical quartz crystal microbalance. *Chem. Soc. Rev.* **2021,** *50*, 10743-10763.

8. Yan, X.; Bain, R. M.; Cooks, R. G., Organic reactions in microdroplets: reaction acceleration revealed by mass spectrometry. *Angew. Chem. Int. Ed.* **2016,** *55*, 12960-12972.

9. Cooks, R. G.; Yan, X., Mass spectrometry for synthesis and analysis. *Annu. Rev. Anal. Chem.* **2018,** *11*, 1-28.

10. Wei, Z.; Li, Y.; Cooks, R. G.; Yan, X., Accelerated reaction kinetics in microdroplets: overview and recent developments. *Annu. Rev. Phys. Chem.* **2020,** *71*, 31-51.

11. Wei, Z.; Zhang, X.; Wang, J.; Zhang, S.; Zhang, X.; Cooks, R. G., High yield accelerated reactions in nonvolatile microthin films: chemical derivatization for analysis of single-cell intracellular fluid. *Chem. Sci.* **2018,** *9*, 7779-7786.

12. Tang, S.; Cheng, H.; Yan, X., On-demand electrochemical epoxidation in nano-electrospray ionization mass spectrometry to locate carbon-carbon double bonds. *Angew. Chem. Int. Ed.* **2020,** *59*, 209-214.

13. Tang, S.; Chen, X.; Ke, Y.; Wang, F.; Yan, X., Voltage-controlled divergent cascade of electrochemical reactions for characterization of lipids at multiple isomer levels using mass spectrometry. *Anal. Chem.* **2022,** *94*, 12750-12756.

14. Wei, Z.; Xie, Z.; Kuvelkar, R.; Shah, V.; Bateman, K.; McLaren, D. G.; Cooks, R. G., High-throughput bioassays using “dip-and-go” multiplexed electrospray mass spectrometry. *Angew. Chem. Int. Ed.* **2019,** *58*, 17594-17598.

15. Kumar, A.; Mondal, S.; Banerjee, S., Aqueous microdroplets capture elusive carbocations. *J. Am. Chem. Soc.* **2021,** *143*, 2459-2463.

16. Kumar, A.; Mondal, S.; Sandeep; Venugopalan, P.; Kumar, A.; Banerjee, S., Destabilized carbocations caged in water microdroplets: isolation and real-time detection of α-carbonyl cation intermediates. *J. Am. Chem. Soc.* **2022,** *144*, 3347-3352.

17. Kumar, A.; Mondal, S.; Mofidfar, M.; Zare, R. N.; Banerjee, S., Capturing reactive carbanions by microdroplets. *J. Am. Chem. Soc.* **2022,** *144*, 7573-7577.

18. Cheng, H.; Yang, T.; Edwards, M.; Tang, S.; Xu, S.; Yan, X., Picomole-scale transition metal electrocatalysis screening platform for discovery of mild C-C coupling and C-H arylation through in situ anodically generated cationic Pd. *J. Am. Chem. Soc.* **2022,** *144*, 1306-1312.

19. Ghosh, J.; Mendoza, J.; Cooks, R. G., Accelerated and concerted Aza-Michael addition and SuFEx reaction in microdroplets in unitary and high-throughput formats. *Angew. Chem. Int. Ed.* **2022,** *61*, e202214090.

20. Cheng, H.; Tang, S.; Yang, T.; Xu, S.; Yan, X., Accelerating electrochemical reactions in a voltage-controlled interfacial microreactor. *Angew. Chem. Int. Ed.* **2020,** *59*, 19862-19867.

21. Gnanamani, E.; Yan, X.; Zare, R. N., Chemoselective *N*-alkylation of indoles in aqueous microdroplets. *Angew. Chem. Int. Ed.* **2020,** *59*, 3069-3072.

22. Basuri, P.; Gonzalez, L. E.; Morato, N. M.; Pradeep, T.; Cooks, R. G., Accelerated microdroplet synthesis of benzimidazoles by nucleophilic addition to protonated carboxylic acids. *Chem. Sci.* **2020,** *11*, 12686-12694.

23. Yan, X.; Cheng, H.; Zare, R. N., Two-phase reactions in microdroplets without the use of phase-transfer catalysts. *Angew. Chem. Int. Ed.* **2017,** *56*, 3562-3565.

24. Liu, C.; Li, J.; Chen, H.; Zare, Richard N., Scale-up of microdroplet reactions by heated ultrasonic nebulization. *Chem. Sci.* **2019,** *10*, 9367-9373.

25. Yan, X.; Lai, Y.-H.; Zare, R. N., Preparative microdroplet synthesis of carboxylic acids from aerobic oxidation of aldehydes. *Chem. Sci.* **2018,** *9*, 5207-5211.

26. Nie, H.; Wei, Z.; Qiu, L.; Chen, X.; Holden, D. T.; Cooks, R. G., High-yield gram-scale organic synthesis using accelerated microdroplet/thin film reactions with solvent recycling. *Chem. Sci.* **2020,** *11*, 2356-2361.

27. Huang, K.-H.; Wei, Z.; Cooks, R. G., Accelerated reactions of amines with carbon dioxide driven by superacid at the microdroplet interface. *Chem. Sci.* **2021,** *12*, 2242-2250.

28. Li, Y.; Mehari, T. F.; Wei, Z.; Liu, Y.; Cooks, R. G., Reaction acceleration at solid/solution interfaces: Katritzky reaction catalyzed by glass particles. *Angew. Chem. Int. Ed.* **2021,** *60*, 2929-2933.

29. Lee, J. K.; Samanta, D.; Nam, H. G.; Zare, R. N., Spontaneous formation of gold nanostructures in aqueous microdroplets. *Nat. Commun.* **2018,** *9*, 1562.

30. Lee, J. K.; Samanta, D.; Nam, H. G.; Zare, R. N., Micrometer-sized water droplets induce spontaneous reduction. *J. Am. Chem. Soc.* **2019,** *141*, 10585-10589.

31. Lee, J. K.; Walker, K. L.; Han, H. S.; Kang, J.; Prinz, F. B.; Waymouth, R. M.; Nam, H. G.; Zare, R. N., Spontaneous generation of hydrogen peroxide from aqueous microdroplets. *Proc. Natl. Acad. Sci. U. S. A.* **2019,** *116*, 19294-19298.

32. Banerjee, S.; Basheer, C.; Zare, R. N., A study of heterogeneous catalysis by nanoparticle-embedded paper-spray ionization mass spectrometry. *Angew. Chem. Int. Ed.* **2016,** *55*, 12807-12811.

33. Luo, K.; Li, J.; Cao, Y.; Liu, C.; Ge, J.; Chen, H.; Zare, R. N., Reaction of chloroauric acid with histidine in microdroplets yields a catalytic Au-$(His)_2$ complex. *Chem. Sci.* **2020,** *11*, 2558-2565.

34. Eremin, D. B.; Fokin, V. V., On-water selectivity switch in microdroplets in the 1,2,3-triazole synthesis from bromoethenesulfonyl fluoride. *J. Am. Chem. Soc.* **2021,** *143*, 18374-18379.

35. Xing, D.; Meng, Y.; Yuan, X.; Jin, S.; Song, X.; Zare, R. N.; Zhang, X., Capture of hydroxyl radicals by hydronium cations in water microdroplets. *Angew. Chem. Int. Ed.* **2022,** *61*, e202207587.

36. Mehrgardi, M. A.; Mofidfar, M.; Zare, R. N., Sprayed water microdroplets are able to generate hydrogen peroxide spontaneously. *J. Am. Chem. Soc.* **2022,** *144*, 7606-7609.

37. Gao, D.; Jin, F.; Lee, J. K.; Zare, R. N., Aqueous microdroplets containing only ketones or aldehydes undergo Dakin and Baeyer-Villiger reactions. *Chem. Sci.* **2019,** *10*, 10974-10978.

38. Zhao, L.; Song, X.; Gong, C.; Zhang, D.; Wang, R.; Zare, R. N.; Zhang, X., Sprayed water microdroplets containing dissolved pyridine spontaneously generate pyridyl anions. *Proc. Natl. Acad. Sci. U. S. A.* **2022,** *119*, e2200991119.

39. Nam, I.; Lee, J. K.; Nam, H. G.; Zare, R. N., Abiotic production of sugar phosphates and uridine ribonucleoside in aqueous microdroplets. *Proc. Natl. Acad. Sci. U. S. A.* **2017,** *114*, 12396-12400.

40. Nam, I.; Nam, H. G.; Zare, R. N., Abiotic synthesis of purine and pyrimidine ribonucleosides in aqueous microdroplets. *Proc. Natl. Acad. Sci. U. S. A.* **2018,** *115*, 36-40.

41. Zhong, X.; Chen, H.; Zare, R. N., Ultrafast enzymatic digestion of proteins by microdroplet mass spectrometry. *Nat. Commun.* **2020,** *11*, 1049.

42. Zhao, P.; Gunawardena, H. P.; Zhong, X.; Zare, R. N.; Chen, H., Microdroplet ultrafast reactions speed antibody characterization. *Anal. Chem.* **2021,** *93*, 3997-4005.

43. Holden, D. T.; Morato, N. M.; Cooks, R. G., Aqueous microdroplets enable abiotic synthesis and chain extension of unique peptide isomers from free amino acids. *Proc. Natl. Acad. Sci. U. S. A.* **2022,** *119*, e2212642119.

44. Gong, C.; Li, D.; Li, X.; Zhang, D.; Xing, D.; Zhao, L.; Yuan, X.; Zhang, X., Spontaneous reduction-induced degradation of viologen compounds in water microdroplets and its inhibition by host-guest complexation. *J. Am. Chem. Soc.* **2022,** *144*, 3510-3516.

45. Banerjee, S.; Gnanamani, E.; Yan, X.; Zare, R. N., Can all bulk-phase reactions be accelerated in microdroplets? *Analyst* **2017,** *142*, 1399-1402.

46. Gao, D.; Jin, F.; Yan, X.; Zare, R. N., Selective synthesis in microdroplets of 2-phenyl-2,3-dihydrophthalazine-1,4-dione from phenyl hydrazine with phthalic anhydride or phthalic acid. *Chem. Eur. J.* **2019,** *25*, 1466-1471.

47. Beletskaya, I. P.; Nájera, C.; Yus, M., Chemodivergent reactions. *Chem. Soc. Rev.* **2020,** *49*, 7101-7166.

48. Wani, I. A.; Bhattacharyya, A.; Sayyad, M.; Ghorai, M. K., Temperature-modulated diastereoselective transformations of 2-vinylindoles to tetrahydrocarbazoles and tetrahydrocycloheptadiindoles. *Org. Biomol. Chem.* **2018,** *16*, 2910-2922.

49. Holt, C.; Alachouzos, G.; Frontier, A. J., Leveraging the *halo*-Nazarov cyclization for the chemodivergent assembly of functionalized haloindenes and indanones. *J. Am. Chem. Soc.* **2019,** *141*, 5461-5469.

50. Balkenhohl, M.; Kölbl, S.; Georgiev, T.; Carreira, E. M., Mn- and Co-catalyzed aminocyclizations of unsaturated hydrazones providing a broad range of functionalized pyrazolines. *JACS Au* **2021,** *1*, 919-924.

51. Nie, S.; Lu, A.; Kuker, E. L.; Dong, V. M., Enantioselective hydrothiolation: diverging cyclopropenes through ligand control. *J. Am. Chem. Soc.* **2021,** *143*, 6176-6184.

52. Lin, J.-P.; Zhang, F.-H.; Long, Y.-Q., Solvent/oxidant-switchable synthesis of multisubstituted quinazolines and benzimidazoles via metal-free selective oxidative annulation of arylamidines. *Org. Lett.* **2014,** *16*, 2822-2825.

53. Tanifuji, R.; Koketsu, K.; Takakura, M.; Asano, R.; Minami, A.; Oikawa, H.; Oguri, H., Chemo-enzymatic total syntheses of jorunnamycin A, saframycin A, and *N*-Fmoc saframycin Y3. *J. Am. Chem. Soc.* **2018,** *140*, 10705-10709.

54. Yang, P.-F.; Liang, J.-X.; Zhao, H.-T.; Shu, W., Access to enantioenriched 1, n-diamines via Ni-catalyzed hydroamination of unactivated alkenes with weakly coordinating groups. *ACS Catal.* **2022,** *12*, 9638-9645.

55. Viso, A.; Fernández de la Pradilla, R.; Tortosa, M.; García, A.; Flores, A., Update 1 of: α, β-diamino acids: biological significance and synthetic approaches. *Chem. Rev.* **2011,** *111*, PR1-PR42.

56. Li, K.; Huang, S.; Liu, T.; Jia, S.; Yan, H., Organocatalytic asymmetric dearomatizing hetero-Diels-Alder reaction of nonactivated arenes. *J. Am. Chem. Soc.* **2022,** *144*, 7374-7381.

57. Zhang, S.; Bedi, D.; Cheng, L.; Unruh, D. K.; Li, G.; Findlater, M., Cobalt(II)-catalyzed stereoselective olefin isomerization: facile access to acyclic trisubstituted alkenes. *J. Am. Chem. Soc.* **2020,** *142*, 8910-8917.

58. Cardona, F.; Goti, A., Metal-catalysed 1,2-diamination reactions. *Nat. Chem.* **2009,** *1*, 269-275.

59. González-Sabín, J.; Rebolledo, F.; Gotor, V., *trans*-Cyclopentane-1,2-diamine: the second youth of the forgotten diamine. *Chem. Soc. Rev.* **2009,** *38*, 1916-1925.

60. Hembury, G. A.; Borovkov, V. V.; Inoue, Y., Chirality-sensing supramolecular systems. *Chem. Rev.* **2008,** *108*, 1-73.

61. Minakata, S.; Miwa, H.; Yamamoto, K.; Hirayama, A.; Okumura, S., Diastereodivergent intermolecular 1,2-diamination of unactivated alkenes enabled by iodine catalysis. *J. Am. Chem. Soc.* **2021,** *143*, 4112-4118.

62. Fu, N.; Sauer, G. S.; Saha, A.; Loo, A.; Lin, S., Metal-catalyzed electrochemical diazidation of alkenes. *Science* **2017,** *357*, 575-579.

63. Kondoh, A.; Kamata, Y.; Terada, M., Synthesis of enantioenriched γ-amino-α,β-unsaturated esters utilizing palladium-catalyzed rearrangement of allylic carbamates for direct application to formal [3 + 2] cycloaddition. *Org. Lett.* **2017,** *19*, 1682-1685.

64. Zhou, M.; Li, K.; Chen, D.; Xu, R.; Xu, G.; Tang, W., Enantioselective reductive coupling of imines templated by chiral diboron. *J. Am. Chem. Soc.* **2020,** *142*, 10337-10342.

65. Pan, H.-J.; Lin, Y.; Gao, T.; Lau, K. K.; Feng, W.; Yang, B.; Zhao, Y., Catalytic diastereo- and enantioconvergent synthesis of vicinal diamines from diols through borrowing hydrogen. *Angew. Chem. Int. Ed.* **2021,** *60*, 18599-18604.

66. Chen, Y.; Pan, Y.; He, Y.-M.; Fan, Q.-H., Consecutive intermolecular reductive amination/asymmetric hydrogenation: facile access to sterically tunable chiral vicinal diamines and *N*-heterocyclic carbenes. *Angew. Chem. Int. Ed.* **2019,** *58*, 16831-16834.

67. Wang, J.; Ye, S.; Liu, X.; Loh, T.-P., Hydrazine as facile nitrogen source for direct synthesis of amines over a supported Pt catalyst. *ACS Sustainable Chem. Eng.* **2020,** *8*, 16283-16295.

68. Lee, B. J.; Ickes, A. R.; Gupta, A. K.; Ensign, S. C.; Ho, T. D.; Tarasewicz, A.; Vanable, E. P.; Kortman, G. D.; Hull, K. L., Synthesis of unsymmetrical vicinal diamines via directed hydroamination. *Org. Lett.* **2022,** *24*, 5513-5518.

69. Wang, Y.; Wang, Q.; Zhu, J., Organocatalytic nucleophilic addition of hydrazones to imines: synthesis of enantioenriched vicinal diamines. *Angew. Chem. Int. Ed.* **2017,** *56*, 5612-5615.

70. Fava, E.; Millet, A.; Nakajima, M.; Loescher, S.; Rueping, M., Reductive umpolung of carbonyl derivatives with visible-light photoredox catalysis: direct access to vicinal diamines and amino alcohols via α-amino radicals and ketyl radicals. *Angew. Chem. Int. Ed.* **2016,** *55*, 6776-6779.

71. Pan, S.; Jiang, M.; Zhong, G.; Dai, L.; Zhou, Y.; Wei, K.; Zeng, X., Visible-light-induced selectivity controllable synthesis of diamine or imidazoline derivatives by multicomponent decarboxylative radical coupling reactions. *Org. Chem. Front.* **2020,** *7*, 4043-4049.

72. Sprague, D. J.; Singh, A.; Johnston, J. N., Diastereo- and enantioselective additions of α-nitro esters to imines for anti-α,β-diamino acid synthesis with α-alkyl-substitution. *Chem. Sci.* **2018,** *9*, 2336-2339.

73. Kano, T.; Sakamoto, R.; Akakura, M.; Maruoka, K., Stereocontrolled synthesis of vicinal diamines by organocatalytic asymmetric mannich reaction of *N*-protected aminoacetaldehydes: formal synthesis of (−)-agelastatin A. *J. Am. Chem. Soc.* **2012,** *134*, 7516-7520.

74. Lillo, V. J.; Mansilla, J.; Saá, J. M., Organocatalysis by networks of cooperative hydrogen bonds: enantioselective direct Mannich addition to preformed arylideneureas. *Angew. Chem. Int. Ed.* **2016,** *55*, 4312-4316.

75. Huang, Y.; Khoury, K.; Chanas, T.; Dömling, A., Multicomponent synthesis of diverse 1,4-benzodiazepine scaffolds. *Org. Lett.* **2012,** *14*, 5916-5919.

76. Yang, Y.; Xu, Y.; Jones, C. R., A ring expansion route to benzofused *N*-heterocycles through aryne insertion into 1,3-diaza-heterocycles. *Eur. J. Org. Chem.* **2019,** *2019*, 5196-5200.

77. Cheng, P.; Zhang, Q.; Ma, Y.-B.; Jiang, Z.-Y.; Zhang, X.-M.; Zhang, F.-X.; Chen, J.-J., Synthesis and in vitro anti-hepatitis B virus activities of 4-aryl-6-chloro-quinolin-2-one and 5-aryl-7-chloro-1,4-benzodiazepine derivatives. *Bioorg. Med. Chem. Lett.* **2008,** *18*, 3787-3789.

78. Azuaje, J.; Pérez-Rubio, J. M.; Yaziji, V.; El Maatougui, A.; González-Gomez, J. C.; Sánchez-Pedregal, V. c. M.; Navarro-Vázquez, A.; Masaguer, C. F.; Teijeira, M.; Sotelo, E., Integrated ugi-based assembly of functionally, skeletally, and stereochemically diverse 1,4-benzodiazepin-2-ones. *J. Org. Chem.* **2015,** *80*, 1533-1549.

79. Fier, P. S.; Whittaker, A. M., An atom-economical method to prepare enantiopure benzodiazepines with *N*-carboxyanhydrides. *Org. Lett.* **2017,** *19*, 1454-1457.

80. Shi, S.; Meng, G.; Szostak, M., Synthesis of biaryls through nickel-catalyzed Suzuki-Miyaura coupling of amides by carbon-nitrogen bond cleavage. *Angew. Chem. Int. Ed.* **2016,** *55*, 6959-6963.

81. Xiong, L.; Deng, R.; Liu, T.; Luo, Z.; Wang, Z.; Zhu, X.-F.; Wang, H.; Zeng, Z., Selective C–N bond cleavage of *N*-acylisatins: towards high performance acylation/arylation/transamination reagents. *Adv. Synth. Catal.* **2019,** *361*, 5383-5391.

82. Pattarawarapan, M.; Yamano, D.; Wiriya, N.; Yimklan, S.; Phakhodee, W., Simultaneous formation and functionalization of aryliminophosphoranes using 1,3-dihydro-1*H*-benzimidazol-2-ones as precursors. *J. Org. Chem.* **2020,** *85*, 13330-13338.

83. Lambert, J. B.; Majchrzak, M. W., Ring-chain tautomerism in 1,3-diaza and 1,3-oxaza heterocycles. *J. Am. Chem. Soc.* **1980,** *102*, 3588-3591.

84. Lambert, J. B.; Wang, G. T.; Huseland, D. E.; Takiff, L. C., Acid-catalyzed ring-chain tautomerism in 1,3-diazolidines. *J. Org. Chem.* **1987,** *52*, 68-71.

85. Zhu, X.; Zhang, W.; Lin, Q.; Ye, M.; Xue, L.; Liu, J.; Wang, Y.; Cheng, H., Direct microdroplet synthesis of carboxylic acids from alcohols by preparative paper spray ionization without phase transfer catalysts. *ACS Sustainable Chem. Eng.* **2019,** *7*, 6486-6491.

86. Müller, T.; Badu-Tawiah, A.; Cooks, R. G., Accelerated carbon–carbon bond-forming reactions in preparative electrospray. *Angew. Chem. Int. Ed.* **2012,** *51*, 11832-11835.

87. Wei, Z.; Wleklinski, M.; Ferreira, C.; Cooks, R. G., Reaction acceleration in thin films with continuous product deposition for organic synthesis. *Angew. Chem. Int. Ed.* **2017,** *56*, 9386-9390.

88. Song, W.; Wang, Y.; Huang, L.; Cheng, H.; Wu, J.; Pan, Y., Reactive paper spray mass spectrometry for rapid analysis of formaldehyde in facial masks. *Rapid Commun. Mass Spectrom.* **2019,** *33*, 1091-1096.

89. Lin, Q.; Sun, J.; Wang, Y.; Ye, M.; Cheng, H., Rapid determination of aldehydes in food by high-throughput reactive paper spray ionization mass spectrometry. *J. Food Compost. Anal.* **2022,** *114*, 104814.